2024 IEEE International Conference on Robotics and Automation (ICRA 2024)
May 13-17, 2024. Yokohama, Japan

A Novel Funnel-Based $\mathcal{L}_1$ Adaptive Fuzzy Approach for the Control Of An Actuated Ankle Foot Orthosis

Oussama Bey[1], Rami Jradi[1], Huiseok Moon[1], Hala Rifaï[1], Kaushik Das Sharma[2], Yacine Amirat[1] and Samer Mohammed[1]

***Abstract*— This paper introduces a novel funnel-based adaptive $\mathcal{L}_1$ fuzzy control strategy for assisting ankle joint movement during walking with the use of an actuated ankle foot orthosis (AAFO). A projection-based adaptation mechanism employing a fuzzy system is used to estimate the unknown time-varying parameters of the $\mathcal{L}_1$ control law, ensuring precise tracking of the AAFO-wearer system by the state estimator. The projection operator guarantees the convergence of the parameters while offering a limited amount of assistance torque. Funnel-based feedback control is used to mitigate the typical time lag seen when using $\mathcal{L}_1$-based approaches due to the presence of a low-pass filter commonly used in this type of approach. The effectiveness of the proposed control strategy is demonstrated through real-time experiments involving five healthy subjects.**

I. INTRODUCTION

The current challenges posed by a rapidly aging global population, coupled with the increasing incidence of strokes, highlight the urgent need to develop effective, efficient, and individualized rehabilitation techniques [1], [2]. Conventional therapeutic strategies often require a significant amount of physical effort and time from healthcare providers, often resulting in insufficient precision and personalization of the rehabilitation process. These concerns are amplified by the dramatic demographic changes currently taking place. More and more people are becoming very vulnerable to factors that can significantly reduce their mobility, such as age-related musculoskeletal degeneration or impairments caused by strokes [3]. Foot drop is a typical example of the impact of neurological or muscular disorders on walking patterns. Foot drop can seriously impair an individual's ability to walk properly, as it impairs dorsiflexion, i.e. the upward movement of the foot at the ankle. The foot and toes then drag, which not only creates an abnormal gait, but also increases the risk of falling. This problem not only limits mobility, but also poses a significant safety risk [4].

An actuated ankle foot orthosis (AAFO) is an interesting solution for treating the effects of foot drop [3]. Unlike their passive counterparts, AAFOs are equipped with motors and sensors, and can be driven using advanced control algorithms. This allows for more controllable and dynamic support, enabling assistance to be tailored to the specific needs of the user. This not only improves rehabilitation results, but also considerably reduces the physical workload on therapists [5]. Instead of being actively involved in manipulating the patient's limbs, healthcare providers can now play a supervisory role, monitoring the rehabilitation session and making any necessary adjustments. The effectiveness of robotic orthoses is highly dependent on their control system, particularly in the context of physical human-robot interaction, an area that has been the subject of extensive research in recent years. Effective control of a robotic orthosis can be achieved through a variety of strategies aimed at correcting the wearer's movement while ensuring the transparency of the orthosis to the wearer. These strategies include EMG-based methods that measure the wearer's muscular effort and use the orthosis to generate the necessary assistance by supplementing the effort required [6], [7]. Another strategy is torque control, which directly controls the torque/force of the motor, allowing the orthosis to precisely generate the torque/force needed to complete the wearer's movement [8], [9]. Impedance-based control methods, which do not rely on predefined trajectories, have also been explored [10], [11]. However, these control methods require the wearer to voluntarily initiate the movement. Although these strategies provide significant assistance to the wearer, their main limitation is their dependence on user-initiated movements. Another method of control consists of following a predefined healthy trajectory. This strategy is particularly suitable for individuals who are unable to initiate movement, as the orthosis can help to achieve the desired movement with precision without depending on the user's initiative [12], [13]. Various control strategies have been proposed in the literature in the context of trajectory following assistance controllers, such as the predictive controllers [14] and the sliding-mode-based controllers [15], [16]. Although the above-mentioned control strategies have proven efficient, as model-based controllers they require prior knowledge of the AAFO-wearer system model through an identification process. Adaptive control has the ability to provide the necessary assistance without requiring prior knowledge of the AAFO-wearer system, as shown in [4], [5], [17].

In this paper, a funnel-based $\mathcal{L}_1$ adaptive fuzzy control is proposed for controlling an actuated ankle-foot orthosis to aid in ankle joint plantarflexion/dorsiflexion movement. The key features of the proposed control strategy are as follows :

1) An $\mathcal{L}_1$ Fuzzy approach is introduced, where a fuzzy system is used to approximate the $\mathcal{L}_1$ adaptive parameters [18]. Unlike traditional $\mathcal{L}_1$ studies that often

[1]Univ Paris Est Creteil, LISSI, F-94400 Vitry, France. E-mails: {oussama.bey, rami.jradi,hala.rifai, amirat, samer.mohammed}@u-pec.fr,huiseok.moon@univ-paris-est.fr
[2] SCL, Dpt. Applied Physics, Univ Calcutta, Kolkata 700009, India. E-mail: kaushikdassharma@yahoo.com

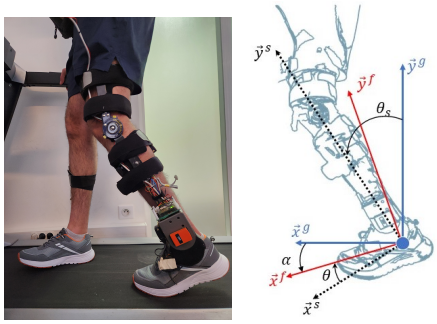

(a) (b)

FIG. 1. View of the AAFO-wearer system [5]. The foot coordinate system $\mathcal{F}(\vec{x}^f, \vec{y}^f, \vec{z}^f)$ is positioned at the ankle, with $\vec{x}^f$ aligned along the heel-toe half of the insole. A static ground coordinate $\mathcal{G}(\vec{x}^g, \vec{y}^g, \vec{z}^g)$ is in place. Angle θ_s is the shank's orientation with respect to the vertical axe $\vec{y}^g$, α defines the foot's alignment, and θ is the angle between the shank and foot.

consider parameters as static [19], [20], [21], [18], [22], the proposed fuzzy adaptation considers these parameters as dynamic, which improves the robustness of the control system with respect to the parametric uncertainties of the model.

2) A projection operator is introduced in the adaptation mechanism to constrain the evolution of the adaptive parameters while ensuring their convergence and enabling the controller to provide the necessary assistive torque to the wearer.

3) Unlike earlier studies [21], [20], [19] which rely on static state feedback, the proposed time-varying funnel-based feedback is integrated into the main $\mathcal{L}_1$ controller. Its goal is to mitigate the usual time lag generated by conventional $\mathcal{L}_1$ control and maintain the tracking error within a predefined range.

The proposed controller is capable of providing controllable assistance without any prior knowledge of the AAFO-wearer system parameters while compensating for external disturbances that may affect the wearer's walking patterns. Compared with our previous work [5], the design and formulation of the proposed controller does not require the use of additional wearable sensors, such as inertial measurement units (IMU) or force-sensitive resistors (FSR). To the best of our knowledge, this is the first study to combine fuzzy system with $\mathcal{L}_1$ adaptive control and a funnel-based approach for the control of a robotic orthosis, in particular an ankle foot orthosis (AAFO). The rest of the paper is structured as follows : Section II presents the dynamic modeling of the ankle orthosis. In Section III, the funnel-based adaptive fuzzy $\mathcal{L}_1$ controller is introduced, with a focus on detailing its design and stability analysis. Section IV presents and analyses the experimental results, while section V concludes the paper and gives future perspectives.

II. AAFO-WEARER MODELLING

In terms of mechanical design, the orthosis has one active degree of freedom at the ankle joint and one passive degree of freedom at the knee joint (Fig. 1). The active DoF is actuated by a geared DC motor with a reduction ratio of 114.4 :1 and weights 3 Kg ; driving the ankle joint to provide assistance for dorsiflexion and plantarflexion with a maximum torque of 10 N.m. An embedded rotary encoder measures the ankle position θ while the ankle velocity, $\dot{\theta}$, is derived numerically. Three force sensitive resistors (FSRs) placed in each shoe's insole are used to detect the gait subphases [5]. The computing unit and the power battery are securely strapped around the waist. The angle α, representing the orientation of the foot with respect to the longitudinal direction, is calculated as follows : $\alpha = \theta_s + \theta$.

The dynamics of the AAFO-wearer system can be expressed as follows :

$$J\ddot{\theta} = \tau_{frc} + \tau_{ac} + \tau_s + \tau_r + \tau_{gr} + \tau_h + \tau \tag{1}$$

where $\ddot{\theta}$ is acceleration of the ankle joint, τ_{frc} is the friction torque (solid and viscous), τ_a is the torque induced by the translational acceleration of the foot, τ_s is the system's joint stiffness torque, τ_r is the torque induced by the ground reaction forces, τ_{gr} is the gravity torque exerted by the foot on the ankle, τ_h is the torque produced by the plantar flexion and dorsiflexion muscle groups, and τ is the torque developed by the AAFO's actuator. These torques can be formulated as follows :

$$\begin{aligned}
\tau_{frc} &= -\gamma_a \operatorname{sign}\dot{\theta} - \gamma_b\dot{\theta}, \\
\tau_{ac} &= -\gamma_c \left(a_y \cos\alpha - a_x \sin\alpha\right), \\
\tau_s &= -\gamma_k \left(\theta - \theta_r\right), \\
\tau_r &= -\gamma_{gr} \left(R_1 x_{gr_1} - R_2 x_{gr_2} - R_3 x_{gr_3}\right) \cos\alpha, \\
\tau_{gr} &= -\tau_g \cos\alpha.
\end{aligned} \tag{2}$$

θ_r is the position of the ankle joint at rest, a_x and a_y are respectively the longitudinal and vertical accelerations associated with the translational movement of both shank and foot, R_1, R_2, R_3 are the ground reaction forces at the heel, middle and toes levels with x_{gr_1}, x_{gr_2}, x_{gr_3} their respective positions. γ_a, γ_b, γ_c, γ_k, γ_{gr} and τ_g are respectively the solid friction, viscous friction, acceleration, stiffness, ground reaction force and gravity system's parameters. sign is a signum function. Let $x = [x_1, x_2] = [\theta, \dot{\theta}]$ be the state vector with $\theta_r = 0$, (1) can be re-written as $\mathcal{L}_1$ state-space system's class as follows :

$$\dot{x} = A_m x + B\left(w\tau + \eta^T x + \sigma\right) \tag{3}$$

where $A_m = A - Bk_m^T$ with $A = \begin{bmatrix} 0 & 1 \\ 0 & 0 \end{bmatrix}$ and $B = \begin{bmatrix} 0 \\ 1 \end{bmatrix}$. $k_m \in \mathbb{R}^{2\times 1}$ is a state vector selected such that A_m is stable. w, η and σ are as follows :

$$\begin{aligned}
w &= J^{-1} \\
\eta &= [-\gamma_k, -\gamma_b]^T \\
\sigma &= J^{-1}\left(\tau_r + \tau_g + \tau_{ac} - \gamma_a \operatorname{sign}(x_2) + \tau_h\right) - k_m x.
\end{aligned}$$

Note that the pair (A, B) is controllable.

III. FUNNEL-BASED $\mathcal{L}_1$ ADAPTIVE FUZZY CONTROLLER DESIGN

The objective is to design an adaptive $\mathcal{L}_1$ control input denoted as τ_d augmented by a funnel based time-varying feedback control τ_f so that the output of the system θ follows

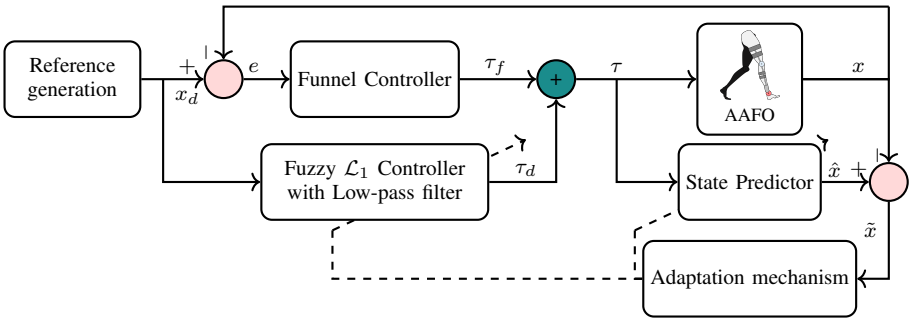

FIG. 2. Proposed Control Framework

precisely the desired trajectory denoted θ_d. Thus, the overall control input can be written as follows :

$$\tau = \tau_d + \tau_f \tag{4}$$

The parameters of the system are estimated using fuzzy system, and then a state predictor is designed based on this estimate to improve adaptation and reduce tracking error. The overall control framework is depicted in Fig. 2.

A. *Adaptive fuzzy L_1 controller*

Unlike traditional $\mathcal{L}_1$ control approaches, the control approach proposed in this paper uses a fuzzy logic system for parameter estimation. thus, we can write the following notation [23] :

$$\begin{aligned} \eta &= W_\eta^{*T}\xi + \varepsilon_\eta \\ w &= W_w^{*T}\xi + \varepsilon_w \\ \sigma &= W_\sigma^{*T}\xi + \varepsilon_\sigma \end{aligned} \tag{5}$$

where W_η^*, W_w^* and W_σ^* are optimal parameter vector. with :

— $\xi(x) = [\xi_1(x) \dots \xi_N(x)]^T$

$\xi_k(x) = \frac{\mu_k(x)}{\sum_{j=1}^N \mu_j(x)}$ with $|\xi_k| \leq 1 \quad \forall k = 1, \dots, N.$

$\mu_k(x) = \prod_{i=1}^n \mu_{\breve{F}_i^k}, \breve{F}_i^k \in \{F_i^1, \dots, F_i^{m_i}\}$ represents the weight of rule R_k. ε_w, ε_θ and ε_σ are too small bounded approximation errors. Using the fuzzy representation, (3) can be rewritten as follows :

$$\dot{x} = Ax + B[W_w^{*T}\xi\tau + W_\eta^{*T}\xi x + W_\sigma^{*T}\xi + \varepsilon] \tag{6}$$

where ε represents the sum of the resulting bounded approximation errors with $|\varepsilon| \leq \bar{\varepsilon}$. It is important to note that the optimal parameter vectors are unknown a priori. Therefore, to overcome this issue, the estimated values are used. Thus :

$$\begin{aligned} \hat{\eta} &= \hat{W}_{\hat{\eta}}\xi \\ \hat{w} &= \hat{W}_{\hat{w}}\xi \\ \hat{\sigma} &= \hat{W}_{\hat{\sigma}}\xi \end{aligned} \tag{7}$$

These estimations are used in the following state predictor :

$$\begin{aligned} \dot{\hat{x}} = A_m\hat{x} + B\big(&\hat{W}_w^T\xi\tau + \hat{W}_\eta^T\xi x + \hat{W}_\sigma^T\xi \\ &- \hat{\bar{\varepsilon}}\,\mathrm{sign}(\tilde{x}^T PB)\big) \end{aligned} \tag{8}$$

$\tilde{x} = x - \hat{x}$ is the prediction error, $\hat{\bar{\varepsilon}}$ is the estimate of $\bar{\varepsilon}$, P is a positive definite matrix and unique solution to the following Lyapunov algebraic equation :

$$A_m^T P - PA_m = -Q \tag{9}$$

Q is a positive definite matrix. The estimated parameters are adjusted to align the state predictor model's output with the system's output. Once this alignment is achieved, the applied control law adapts to changes or uncertainties in the system, maintaining robustness and stability. The adaptation mechanism of the estimated parameters can be formulated as follows :

$$\begin{aligned} \dot{\hat{W}}_\eta &= \Gamma_\eta \,\mathrm{Proj}\left(\hat{W}_\eta, -\tilde{x}^T Pb\xi x\right) \\ \dot{\hat{W}}_\sigma &= \Gamma_\sigma \,\mathrm{Proj}\left(\hat{W}_\sigma, -\tilde{x}^T Pb\xi\right) \\ \dot{\hat{W}}_w &= \Gamma_w \,\mathrm{Proj}\left(\omega_w, -\tilde{x}^T Pb\xi\tau\right) \\ \dot{\hat{\bar{\varepsilon}}} &= \Gamma_\varepsilon \,\mathrm{Proj}\left(\hat{\bar{\varepsilon}}, -\left|\tilde{x}^T PB\right|\right) \end{aligned} \tag{10}$$

$\mathrm{Proj}(\hat{W}, y)$ is a projection operator defined in [5]. It is formulated as follows :

$$\mathrm{Proj}(\hat{W}, y) = \begin{cases} y & \text{if } ||\hat{W}|| < W_M \text{ or } \hat{W}^T y \geq 0 \\ (I - \frac{\hat{W}\hat{W}^T}{||\hat{W}||^2})y & \text{if } ||\hat{W}|| \geq W_M \text{ and } \hat{W}^T y < 0 \end{cases} \tag{11}$$

The projection operator has the following properties [5] :

1) $\hat{W}(t)$ is uniformly continuous,
2) If $||\hat{W}(0)|| \leq W_M$, then $||\hat{W}(t)|| \leq W_M$, $\forall t > 0$,
3) $||\mathrm{Proj}(\hat{W}, y)|| \leq ||y||$,
4) $\tilde{W}^T \mathrm{Proj}(\hat{W}, y) \leq \tilde{W}^T y$,
5) $||\mathrm{Proj}(\hat{W}, y)||$ is bounded if $||\hat{W}||$ is also bounded.

Remark 1: Note that the adaptive parameters are estimated so that the dynamics of the state estimator closely match that of the real system, thus improving trajectory tracking. The control law τ_d as shown in 2 can be expressed as follows :

$$\tau_d = -kC(s)\left(\hat{\eta}_l - k_g x_d\right) \tag{12}$$

where $C(s)$ is a bounded input, bounded output stable and strictly proper transfer function, $\hat{\eta}_l(t) = \hat{W}_\eta^T\xi x + \hat{W}_\sigma\xi$, $k_g = -\frac{1}{CA_m^{-1}B}$ is the inverse dc-gain constant, x_d is the reference trajectory and k is a constant gain. The controller defined in (12) guarantees bounded-input bounded-state stability of the system with respect to the reference trajectory and initial conditions if k_m and $C(s)$ verify the following $\mathcal{L}_1$ norm condition :

$$\|G(s)\|_{\mathcal{L}_1} L < 1$$

with $G(s) = H(s)(1 - C(s)), H(s) = (s\mathbb{I} - A_m)^{-1} B$, and $L = \max\{\|\hat{W}_\theta\|, \|\hat{W}_\sigma\|\}$. $G(s), H(s)$ and $C(s)$ are bounded-input bounded-output stable transfer functions, L is the maximum bound set on the parameters $\hat{W}_\theta$ and $\hat{W}_\sigma$.

B. Funnel control design

To solve the time-lag problem that often occurs in $\mathcal{L}_1$ controllers, a funnel control law, τ_f, a time-variant feedback law, is introduced. This law depends on the system's relative degree, as demonstrated in [24]. The main goal here is to design a predefined regime in which the position error remains confined within a boundary funnel. Given that the relative degree of the system considered in this study is 2, according to [24] the control input τ_f takes the following form :

$$\begin{aligned} \tau_f &= -k_1(t)\left(\dot{e}(t) + k_0(t)e(t)\right) \\ k_0(t) &= \frac{1}{1 - \varphi_0^2(t)\|e(t)\|^2} > 0 \\ k_1(t) &= \frac{1}{1 - \varphi_1^2(t)\left\|\dot{e}(t) + k_0(t)e(t)\right\|^2} > 0 \end{aligned} \tag{13}$$

where $e(t) = x_1 - x_d$ is the tracking error, φ_0 and φ_1 are the funnel functions of the position error and its derivative respectively. These two functions are selected to achieve a specific output behavior. In practice, these functions can be of the same type. A common choice can be :

$$\varphi_i^{-1} = \lambda_0 e^{-at} + \lambda_\infty \tag{14}$$

λ_0 denotes the beginning of the funnel functions and λ_∞ is the permanent regime value ; the values of these parameters are chosen a priori. Since k_0 and k_1 are always positive, the funnel controller consistently maintains system stability, as demonstrated in [24].

On the basis of all of these results, the global control input can be written as follows :

$$\tau = -kC(s)\left(\hat{\eta}_l - k_g x_d\right) - k_1\left(\dot{e} + k_0 e\right) \tag{15}$$

C. Stability analysis

To study the stability of the system, the dynamics of the estimation error is obtained by subtracting (5) from (14). The estimation $\dot{\hat{x}}$ is defined as follows :

$$\begin{aligned} \dot{\tilde{x}} =& A_m\tilde{x} + B\big(\tilde{W}_w^T\xi\tau + \tilde{W}_\eta^T\xi x + \tilde{W}_\sigma^T\xi + \varepsilon \\ & - \hat{\bar{\varepsilon}}\,\mathrm{sign}(\tilde{x}^T PB)\big) \end{aligned} \tag{16}$$

Let us choose the following Lyapunov function :

$$\begin{aligned} V =& \frac{1}{2}\tilde{x}^T P\tilde{x} + \frac{1}{2\Gamma_\eta}\tilde{W}_\eta^T\tilde{W}_\eta + \frac{1}{2\Gamma_w}\tilde{W}_w^T\tilde{W}_w + \frac{1}{2\Gamma_\sigma}\tilde{W}_\sigma^T\tilde{W}_\sigma \\ & + \frac{1}{2\Gamma_\epsilon}\tilde{\bar{\varepsilon}}^2 \end{aligned} \tag{17}$$

The time derivative of V can be written as follows :

$$\begin{aligned} \dot{V} =& -\tilde{x}^T Q\tilde{x} + \tilde{x}^T PB\big(\tilde{W}_w^T\xi\tau + \tilde{W}_\eta^T\xi x + \tilde{W}_\sigma^T\xi + \varepsilon \\ & - \hat{\bar{\varepsilon}}\,\mathrm{sign}(\tilde{x}^T PB)\big) + \frac{1}{\Gamma_\eta}\tilde{W}_\eta^T\dot{\hat{W}}_\eta + \frac{1}{\Gamma_w}\tilde{W}_w^T\dot{\hat{W}}_w \\ & + \frac{1}{\Gamma_\sigma}\tilde{W}_\sigma^T\dot{\hat{W}}_\sigma + \frac{1}{\Gamma_\epsilon}\tilde{\bar{\varepsilon}}\dot{\hat{\bar{\varepsilon}}} \end{aligned} \tag{18}$$

After simplification and taking into account that $x\,\mathrm{sign}(x) = |x|, \forall x \in \mathbb{R}$, we obtain :

$$\begin{aligned} \dot{V} \leq & -\tilde{x}^T Q\tilde{x} + \left|\tilde{x}^T PB\right|\bar{\varepsilon} - \hat{\bar{\varepsilon}}\left|\tilde{x}^T PB\right| \\ & + \tilde{x}^T PB\tilde{W}_w^T\xi\tau + \frac{1}{\Gamma_w}\tilde{W}_w^T\dot{\hat{W}}_w + \tilde{x}^T PB\tilde{W}_\eta^T\xi x \\ & + \frac{1}{\Gamma_\eta}\tilde{W}_\eta^T\dot{\hat{W}}_\eta + \tilde{x}^T PB\tilde{W}_\sigma\xi + \frac{1}{\Gamma_\sigma}\tilde{W}_\sigma^T\dot{\hat{W}}_\sigma + \frac{1}{\Gamma_\epsilon}\tilde{\bar{\varepsilon}}\dot{\hat{\bar{\varepsilon}}} \end{aligned} \tag{19}$$

Introducing the adaptation mechanism in (19) and using the projection-based features [25], we obtain :

$$\begin{aligned} \dot{V} \leq & -\tilde{x}^T Q\tilde{x} + \underbrace{\tilde{x}^T PB\tilde{W}_w^T\xi\tau + \tilde{W}_w^T\,\mathrm{Proj}\left(\hat{W}_\omega, -\tilde{x}^T PB\xi\tau\right)}_{\leq 0} \\ & + \underbrace{\tilde{x}^T PB\tilde{W}_\eta^T\xi x + \tilde{W}_\eta^T\,\mathrm{Proj}\left(\hat{W}_\eta, -\tilde{x}^T PB\xi x\right)}_{\leq 0} \\ & + \underbrace{\tilde{x}^T PB\tilde{W}_\sigma\xi + \tilde{W}_\sigma^T\,\mathrm{Proj}\left(\hat{W}_\sigma, -\tilde{x}^T Pb\xi\right)}_{\leq 0} \\ & + \underbrace{\tilde{\bar{\varepsilon}}\left|\tilde{x}^T PB\right| + \tilde{\bar{\varepsilon}}\,\mathrm{Proj}\left(\hat{\bar{\varepsilon}}, -\left|\tilde{x}^T PB\right|\right)}_{\leq 0} \end{aligned} \tag{20}$$

Finally, $\dot{V}$ is reduced to :

$$\dot{V} \leq -\tilde{x}^T Q\tilde{x} \leq 0 \tag{21}$$

and therefore $V \in L_\infty$ and the variables $\tilde{x}_i, \dot{\tilde{x}}_i, x_i, \dot{x}_i, \tilde{W}_\eta, \tilde{W}_\sigma, \tilde{W}_w$ are bounded. Applying the Barbalat's lemma, we can conclude that all the elements constituting the Lyapunov function are asymptotically convergent. This result shows that the predictor model is also stable since all its right-hand side variables are bounded, and since $\tilde{x} = \hat{x} - x$, x is also stable, and therefore, the overall closed-loop system is stable.

IV. Experimental Results

A. Experimental protocol

Five healthy individuals participated in the study (Aged 25±2 years with an average weight of 70±3 kg). They were informed and consented to the experiment. Each subject was asked to walk on the treadmill at a speed of 2 km/h. A series of two unassisted sessions followed by two assisted ones were conducted for one minute each with a one minute rest between sessions. Before each session, five gait cycles gait cycles were used to calibrate the gait subphases detection algorithm to generate the adaptive reference trajectory [4]. During the assisted sessions, the assistance torque is first applied during the stance phase so that any sudden change in the ankle joint position does not affect the wearer's balance and safety. It should be noted that the FSRs are used independently to generate the adaptive reference trajectory.

B. Controller parameters

The controller parameters are chosen as follows : $k_m = [-5, -12]^T$, $kg = 5$, $k = 0.46$, $\Gamma_\sigma = 80.06, \Gamma_\omega = 20.5, \Gamma_\eta = [32.5, 32.5]^T$ and $P = \begin{bmatrix} 62.5 & -25 \\ -25 & 12.5 \end{bmatrix}$ for

Q =diag(50,50); the maximum bound of the projection is set to 50. The filter G is chosen as follows : $G(s) = \frac{25}{s+25}$ and was implemented in real time using discrete variable z^{-1} as $G(z^{-1}) = \frac{25}{1-z^{-1}e^{-25T}}$ where T is the sampling time. Funnel parameters are chosen as follows : $\lambda_0 = 0.08$ and $\lambda_\infty = 0.01$ with $a_1 = 2$ and $a_2 = 2.3$. The vector $[e, \dot{e}]$ represents the input of the fuzzy system. Five Gaussian membership functions are associated with each input variable where $\mu_{F_i^1}(x_i) = \exp\left\{-\frac{1}{2}\left(\frac{x_i - C_i}{\sigma}\right)^2\right\}, \quad i = 1:5$, with centers $C_i = [-1, -0.5, 0, 0.5, 1]$ and a variance equal to $\sigma = 1.6$. Initial values of the adaptive parameters were set as follows : $\hat{W}_\sigma(0) = 0.5 \cdot rand(25,1), \hat{W}_\omega(0) = 7 \cdot rand(25,1), \hat{W}_{x_1}(0) = 7 \cdot rand(25,1), \hat{W}_{x_2}(0) = -1 \cdot rand(25,1)$. Note that these parameters are chosen by the empirical trial and error method to achieve the best possible tracking while maintaining the comfort of the wearer.

C. Results

Fig. 3 provides a comparative analysis of the tracking performance for Subject A with assistance during the first 40 seconds of the experiment. The figure clearly shows that the tracking error is minimized and good tracking performance is achieved with 2.92° error, while maintaining a smooth velocity. A positive torque indicates a dorsiflexion assistance while a negative one represents plantarflexion assistance. One can note the convergence of the adaptive parameters and that the projection operator maintains the norm $\left|\left|\hat{W}_{x_2}\right|\right|$ below the bound W_m

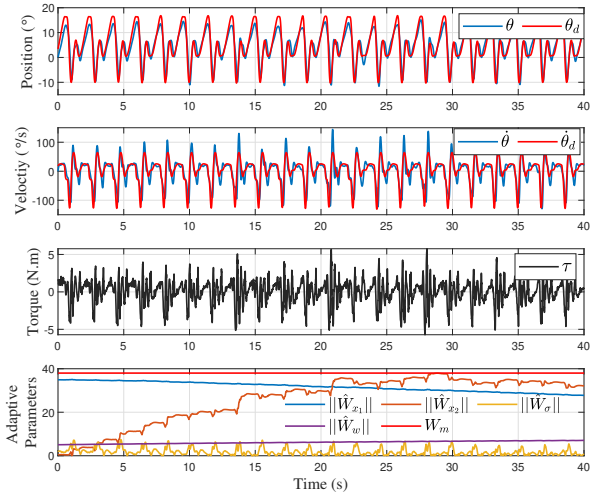

FIG. 3. Subject A. Tracking performances with assistance

Fig. 4 shows that the predicted states closely align with the real ones.

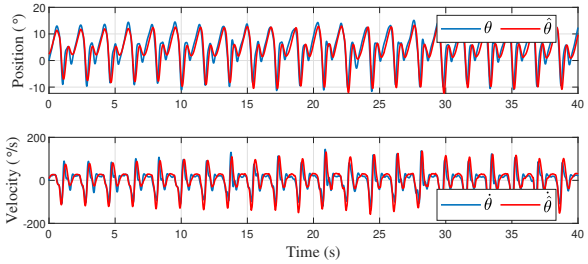

FIG. 4. Subject A : Real-time state estimation

Fig. 5 shows the effectiveness of the controller in dealing with external disturbances resulting from abnormal walking patterns. For this experiment, the subject's knee was mechanically constrained to prevent knee motion, and he was asked to imitate an individual suffering from foot drop by letting his foot fall during the swing phase. Two test sessions were conducted to assess the controller's impact.

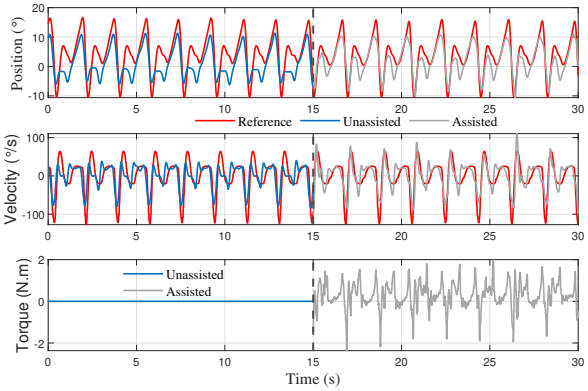

FIG. 5. Subject A : Abnormal walking pattern without and with controller

The use of the proposed controller resulted in a significant improvement in ankle movement, particularly during the swing phase. It can be seen that the correction of the movement occurred at the beginning of dorsiflexion and extended throughout the plantarflexion movement. The correction can be quantified using the position error, which has been significantly reduced from 6.3° to 4.3°.

A full evaluation of the proposed approach has been carried out for subject A through a rigorous comparison with two state-of-the-art adaptive controllers. Fig. 6 shows the average tracking performance for subject A, obtained with the method proposed in [4] and the one presented in [5].

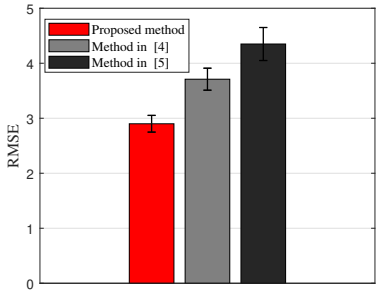

FIG. 6. Subject A : Comparison performance with state-of-the-art methods

One can clearly observe that the proposed approach outperforms state-of-the-art methods in terms of tracking precision. Unlike the methods in [4] and [5], the proposed controller shows better tracking performance since the tracking error is further reduced once the adaptive parameters converge to stable values. Compared to the adaptive control approach described in [4], which fails to reject disturbances and doesn't ensure the convergence of estimated parameters, the method proposed in this paper provides effective compensation for external system disturbances and guarantees parameter convergence via a projection operator. Additionally, the control strategy outlined in [5] achieves similar outcomes but

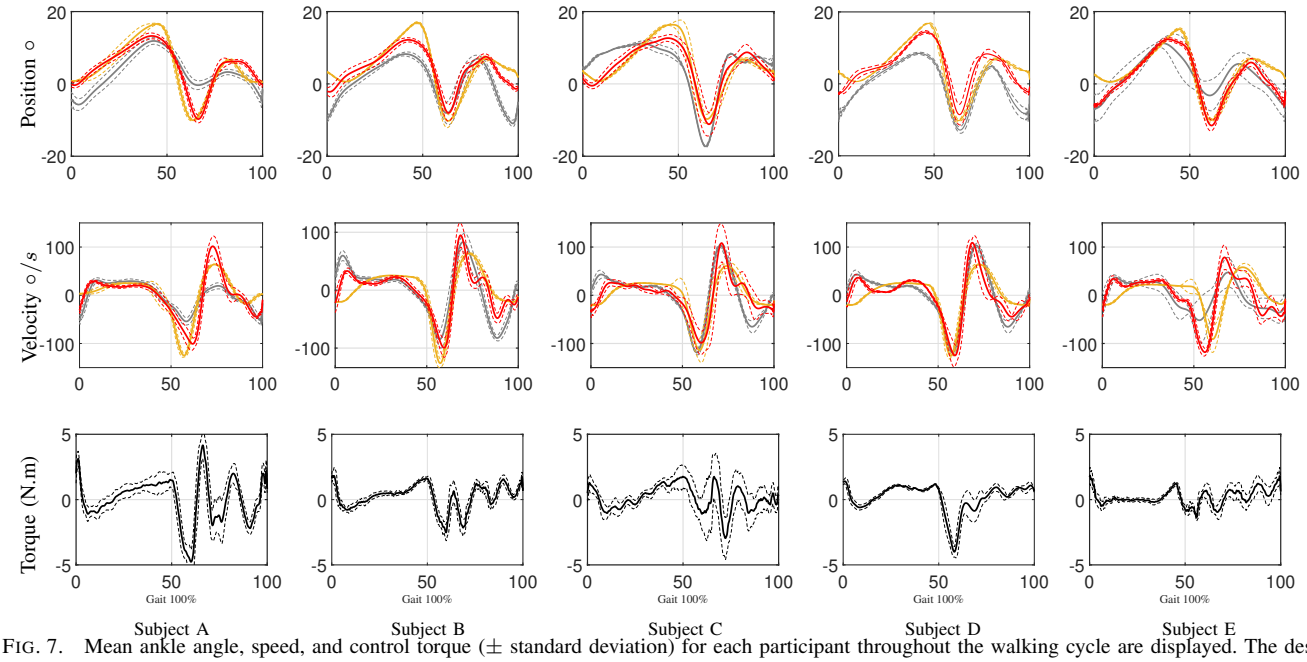

FIG. 7. Mean ankle angle, speed, and control torque (± standard deviation) for each participant throughout the walking cycle are displayed. The desired trajectory is shown by the yellow line, the red line indicates the controlled state using the proposed method, and the gray line shows the state without any assistance.

requires extra sensors such as IMUs and FSRs, a requirement not present in the approach proposed here.

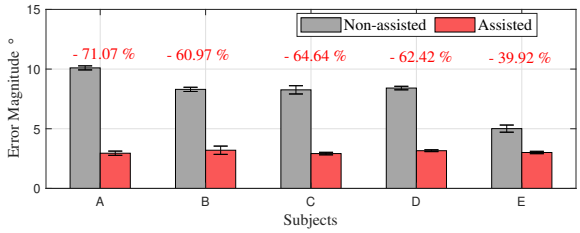

FIG. 8. The mean position tracking error for all subjects

The average position and velocity tracking outcomes, along with the assistance torque for each participant, are depicted in Figure 7. In both assisted and unassisted modes, all subjects exhibited marked improvement in ankle joint positioning. For subjects A and E, assistance was specifically targeted at plantarflexion during push-off and dorsiflexion during the swing phase, aligning the ankle position with the reference trajectory. Subjects B and D received assistance in dorsiflexion, resulting in ankle positioning that adhered to the reference trajectory throughout both the stance and swing phases. Subject C demonstrated comparable tracking performance. While the assistance torque varied among individuals, it remained uniformly smooth and consistent. The gait cycle correction is measured using the root mean squared error (RMSE). Figure 8 presents the RMSE values for ankle joint angles in both assisted and unassisted sessions, highlighting a substantial reduction in RMSE.

V. CONCLUSION

In this paper, a funnel-based $\mathcal{L}_1$ adaptive fuzzy control approach for an actuated ankle-foot orthosis is proposed, with the aim of assisting plantarflexion/dorsiflexion movements of the ankle joint. The control scheme integrates a fuzzy system with a projection-based adaptation mechanism to estimate the system parameters and enhance the effectiveness of AAFO control. To tackle the time-lag intrinsic to $\mathcal{L}_1$ controllers, an auxiliary funnel-based adaptive feedback controller is incorporated into the main control framework. The resulting controller ensures that the position error remains within a specified range, enhancing overall performance. The stability analysis proved that the closed-loop system exhibits bounded-input, bounded-output (BIBO) stability. Experiments involving five healthy subjects demonstrated the effectiveness of the proposed approach in generating real-time reference trajectories customized to individual walking speeds and gait phase durations. Furthermore, it demonstrated superior performance in trajectory tracking and robustness against external disturbances from abnormal walking patterns when compared to state-of-the-art adaptive control approaches. For future research, it would be interesting to extend this control approach to all parts of a lower-limb exoskeleton (hip, knee, ankle) and assess its effectiveness on real patients, considering various lower-limb movements such as walking on level ground, ascending and descending stairs, and transitioning between sitting and standing positions, among others.

REFERENCES

[1] J. M. Ortman, V. A. Velkoff, H. Hogan *et al.*, "An aging nation : the older population in the united states," 2014.

[2] Y. Jiao, Y.-W. Liu, W.-G. Chen, and J. Liu, "Neuroregeneration and functional recovery after stroke : Advancing neural stem cell therapy toward clinical application," *Neural Regeneration Research*, vol. 16, no. 1, p. 80, 2021.

[3] S. A. Roelker, M. G. Bowden, S. A. Kautz, and R. R. Neptune, "Paretic propulsion as a measure of walking performance and functional motor recovery post-stroke : a review," *Gait & posture*, vol. 68, pp. 6–14, 2019.

[4] V. Arnez-Paniagua, H. Rifaï, Y. Amirat, M. Ghedira, J. Gracies, and S. Mohammed, "Adaptive control of an actuated ankle foot orthosis for paretic patients," *Control Engineering Practice*, vol. 90, pp. 207–220, 2019.

[5] R. Jradi, H. Rifai, Y. Amirat, and S. Mohammed, "Adaptive based assist-as-needed control strategy for ankle movement assistance," in *2023 IEEE International Conference on Robotics and Automation (ICRA)*. IEEE, 2023, pp. 12 672–12 678.

[6] E. Trigili, L. Grazi, S. Crea, A. Accogli, J. Carpaneto, S. Micera, N. Vitiello, and A. Panarese, "Detection of movement onset using emg signals for upper-limb exoskeletons in reaching tasks," *Journal of neuroengineering and rehabilitation*, vol. 16, pp. 1–16, 2019.

[7] B. Treussart, F. Geffard, N. Vignais, and F. Marin, "Controlling an upper-limb exoskeleton by emg signal while carrying unknown load," in *2020 IEEE International Conference on Robotics and Automation (ICRA)*. IEEE, 2020, pp. 9107–9113.

[8] G. Aguirre-Ollinger, A. Narayan, and H. Yu, "Phase-synchronized assistive torque control for the correction of kinematic anomalies in the gait cycle," *IEEE Transactions on Neural Systems and Rehabilitation Engineering*, vol. 27, no. 11, pp. 2305–2314, 2019.

[9] G. G. Pena, L. J. Consoni, W. M. dos Santos, and A. A. Siqueira, "Feasibility of an optimal emg-driven adaptive impedance control applied to an active knee orthosis," *Robotics and Autonomous Systems*, vol. 112, pp. 98–108, 2019.

[10] ——, "Feasibility of an optimal emg-driven adaptive impedance control applied to an active knee orthosis," *Robotics and Autonomous Systems*, vol. 112, pp. 98–108, 2019.

[11] M. A. Alouane, H. Rifai, K. Kim, Y. Amirat, and S. Mohammed, "Hybrid impedance control of a knee joint orthosis," *Industrial Robot : the international journal of robotics research and application*, vol. 46, no. 2, pp. 192–201, 2019.

[12] O. Bey, M. Chemachema, Y. Amirat, G. Fried, and S. Mohammed, "Direct adaptive fuzzy-based neural network controller for a human-driven knee joint orthosis," in *2023 American Control Conference (ACC)*. IEEE, 2023, pp. 4677–4682.

[13] Y. Yang, Y. Li, X. Liu, and D. Huang, "Adaptive neural network control for a hydraulic knee exoskeleton with valve deadband and output constraint based on nonlinear disturbance observer," *Neurocomputing*, vol. 473, pp. 14–23, 2022.

[14] B. DeBoer, A. Hosseini, and C. Rossa, "Model predictive control of an active ankle-foot orthosis with non-linear actuation constraints," *Control Engineering Practice*, vol. 136, p. 105538, 2023.

[15] A. Bagheri, D. Dorostkar, M. R. Zakerzadeh, M. J. Sadigh, and M. Mahjoob, "Assessment of the adaptive sliding mode control of an active ankle foot orthosis with an impedance reference," in *2019 7th International Conference on Robotics and Mechatronics (ICRoM)*. IEEE, 2019, pp. 503–507.

[16] H. S. Choi, C. H. Lee, and Y. S. Baek, "Design and validation of a two-degree-of-freedom powered ankle-foot orthosis with two pneumatic artificial muscles," *Mechatronics*, vol. 72, p. 102469, 2020.

[17] R. Jradi, H. Rifaï, and S. Mohammed, "Adaptive active disturbance rejection control of an actuated ankle foot orthosis for ankle movement assistance," *IEEE Robotics and Automation Letters*, 2024.

[18] C. Cao and N. Hovakimyan, "Design and analysis of a novel l_1 adaptive control architecture with guaranteed transient performance," *IEEE Transactions on Automatic Control*, vol. 53, no. 2, pp. 586–591, 2008.

[19] F. Raza, A. Chemori, and M. Hayashibe, "A new augmented l 1 adaptive control for wheel-legged robots : Design and experiments," in *2022 American Control Conference (ACC)*. IEEE, 2022, pp. 22–27.

[20] L. Chikh, A. Chemori, and S. Wang, "Multivariable l1 adaptive depth and attitude control of meros underwater robot with real-time experiments," *IFAC-PapersOnLine*, vol. 55, no. 38, pp. 67–72, 2022.

[21] H. Rifaï, M. B. Abdessalem, A. Chemori, S. Mohammed, and Y. Amirat, "Augmented- 1 adaptive control of an actuated knee joint exoskeleton : From design to real-time experiments," in *2016 IEEE International Conference on Robotics and Automation (ICRA)*. IEEE, 2016, pp. 5708–5714.

[22] N. Hovakimyan, C. Cao, E. Kharisov, E. Xargay, and I. M. Gregory, "L 1 adaptive control for safety-critical systems," *IEEE Control Systems Magazine*, vol. 31, no. 5, pp. 54–104, 2011.

[23] A. Bounemeur and M. Chemachema, "General fuzzy adaptive fault-tolerant control based on nussbaum-type function with additive and multiplicative sensor and state-dependent actuator faults," *Fuzzy Sets and Systems*, p. 108616, 2023.

[24] T. Berger, H. H. Lê, and T. Reis, "Funnel control for nonlinear systems with known strict relative degree," *Automatica*, vol. 87, pp. 345–357, 2018.

[25] G. S. Natal, A. Chemori, and F. Pierrot, "Nonlinear control of parallel manipulators for very high accelerations without velocity measurement : stability analysis and experiments on par2 parallel manipulator," *Robotica*, vol. 34, no. 1, pp. 43–70, 2016.